

Curing Kinetics of Diglycidyl Ether of Bisphenol-A ($n = 0$) Using an Iron-Containing Porphyrin as Cross-Linking Agent

Eva C. Vázquez, Francisco Fraga, J. M. Martínez-Ageitos, José Vázquez Tato

Universidad de Santiago de Compostela, Campus de Lugo, Facultad de Ciencias, Avda Alfonso X el Sabio s/n, 27002 Lugo, Spain
 Correspondence to: J. V. Tato (E-mail: jose.vazquez@usc.es)

ABSTRACT: The curing reaction of a system consisting of a diglycidyl ether of bisphenol-A ($n = 0$) and hemin (a protoporphyrin IX containing an iron ion and an additional chloride ligand) was studied with a differential scanning calorimeter. A maximum value of $-488.3 \pm 8.4 \text{ J g}^{-1}$ was obtained for the enthalpy of the reaction. The kinetics of the process was studied by the isothermal method, observing that it obeys to Kamal's model, with an overall reaction order equal to 3. From the dependence of the kinetic constant with temperature, the activation energy, activation enthalpy, and activation entropy were determined. The ratio of the kinetic constants associated to the autocatalytic and n th order terms of the reaction rate, together with the thermodynamic activation parameters suggest a trend to the autocatalytic path mechanism with increasing temperatures. This study demonstrates that macrocycles can be used as cross-linking agents for curing epoxy resins and that when metallomacrocycles are used, metal ions can be introduced into the network structure. © 2013 Wiley Periodicals, Inc. *J. Appl. Polym. Sci.* 130: 3972–3978, 2013

KEYWORDS: kinetics; thermal properties; resins

Received 11 March 2013; accepted 12 June 2013; Published online 3 July 2013

DOI: 10.1002/app.39659

INTRODUCTION

Cross-linked epoxy resins are nowadays standard options for a variety of applications such as coatings, adhesives, laminates, encapsulations, etc. This is due to their chemical resistance properties, adhesion, no emission of volatile products in the polymerization reaction, versatility in the election of monomers and cross-linkers, low contraction during polymerization, very high adhesion to a variety of surfaces, high mechanical modulus, low creep, and reasonable elevated temperature performance.¹ Epichlorohydrin and bisphenol A diglycidyl ether are among the most common epoxy monomers. Most of the epoxy resins used in coating applications are based on bisphenol A glycidyl ether resins.²

The properties and performance of a cured epoxy polymer are all dependent on the types of epoxy resin, curing agent, and the curing conditions used. The epoxide ring of the monomers can react with chemicals such as alcohols, amines, carboxylic acids, etc., primary and secondary amines being the most widely used curing agents. Examples of polymerization of [diglycidyl ether of bisphenol-A (BADGE), $n = 0$; Figure 1] with diamines have been thoroughly studied by this research group^{3–5} and others.^{6–8} The reaction of bisphenol A diglycidyl ether with diacids is known from long time ago,^{9,10} and many examples have been described in the literature.^{11–19} The subject has been reviewed by Blank et al.² This ring-opening reaction does not produce reactive volatiles and the cross-links formed are stable linkages

with excellent chemical resistance properties.² Reaction of bisphenol A diglycidyl ether with amino and acid bifunctionalized derivatives has also been studied.²⁰

From the synthesis of crown ethers by Pedersen,²¹ macrocyclic compounds have been used for many purposes^{22,23} as, for instance, solubilization of ions in apolar organic solvents. The number or complexing macrocycles has grown considerably and many of them are inspired in natural products as the heme group. All heme proteins contain a tetrapyrrole macrocycle (porphyrin) which is essentially a planar and chemically stable structure. As a result of the four pyrrole nitrogen atoms, porphyrins are tetradentate chelate ligands for metal ions and the resulting metallomacrocyclic is more specifically called a metalloporphyrin or a heme. An example is hemin which is a protoporphyrin IX containing an iron ion and an additional chloride ligand (Figure 1). Porphyrins and metalloporphyrins provide an extremely versatile synthetic moiety for a variety of materials and applications as in photodynamic therapy,²⁴ for designing supramolecular materials,²⁵ and as building blocks for tailored materials properties.²⁶ For instance, they have been used to emulate natural light-harvesting complexes.^{27,28}

The aim of this work is to illustrate that macrocycles can be used as cross-linking agents for curing epoxy resins, and that when metallomacrocyclics are used, the reaction allows the introduction of metal ions in the network structure. For this purpose hemin has been chosen as the cross-linking agent as it

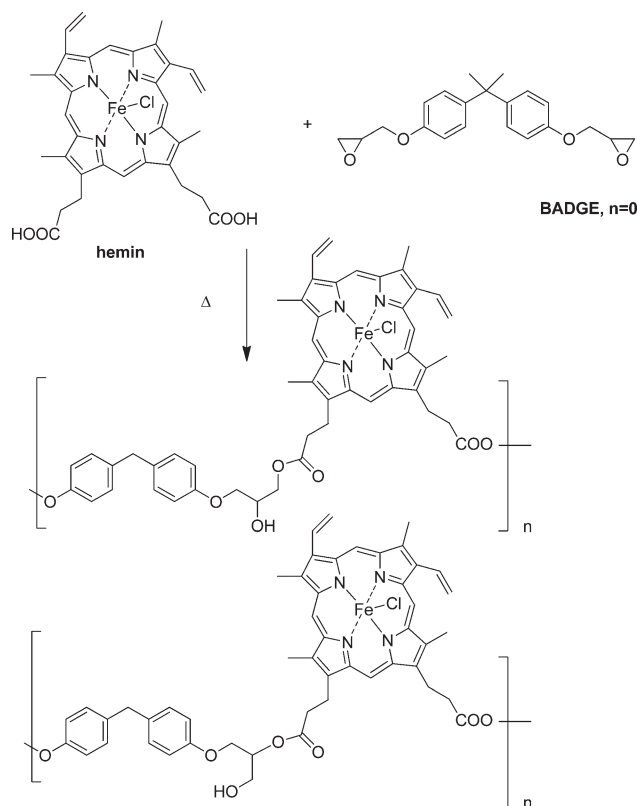


Figure 1. Structure of the materials used in this study: hemin and (BADGE, $n = 0$). Scheme of the formation of the epoxy–hemin resin.

is commercially available, has two free carboxylic groups, and its particular structure allows the change of the central ion. Changing the metal ion will allow to check its possible influence on the properties of the epoxy material in comparative studies. Obviously, metallomacrocycles as cross-linking agents can offer the advantage of a confined ion, while the organic functionalities of the macrocycle may be used for the curing process.

Metal ions have been incorporated into commercial epoxy resins by using transition metal complexes as controllable curing agents,²⁹ diamine derivatives being typical ligands in these complexes.^{30–34} It has been shown that these metal chelate–epoxy polymers have superior thermal stability,^{35–37} the subject being reviewed by Kurnoskin.³⁸ Dicarboxylate ferrocene derivatives have also been studied by non-isothermal measurements and both the diffusion of the compound and the curing temperature affect the curing process.³⁹

These mentioned studies suggest that, as cross-linking agents for epoxy resins, metallomacrocycles can lead to (1) more high-temperature stability resins or increasing toughness, (2) new materials with interesting harvesting properties, (3) the introduction metal ions in the resin structure for modifying the dielectric properties, and (4) improvement the adhesion to metals.⁴⁰

EXPERIMENTAL

Materials and Sample Preparation

The epoxy resin was BADGE (Aldrich). The curing agent used here was hemin (Aldrich) (see Figure 1). Both compounds were

used as received. In the reaction of the epoxy group with a carboxyl group, two different reaction esters may be formed depending on the oxirane ring opening.² One is the ester of the primary hydroxyl group, and the other one is the ester of the secondary hydroxyl group. Although, as a rule of thumb under acidic conditions, the nucleophile attacks the more substituted end, Figure 1 shows both possibilities. What is important is that any of them leads to the growth of the polymer irrespective of the site binding.

In a typical experiment, (BADGE, $n = 0$; 0.100 g, 2.94×10^{-4} mol) and hemin (0.032 g, 8.9×10^{-5} mol; for this example the molar ratio is 6 : 1) were carefully and homogeneously mixed at room temperature. In the second step, a sample of this mixture (typically 8–10 mg) was encapsulated in aluminum pans for the differential scanning calorimeter (DSC) analysis. The optimum (BADGE, $n = 0$)/hemin ratio was determined by running curing experiments at different values of the epoxy/curing agent ratio by the dynamic method.

Techniques

DSC, both in dynamic and in isothermal modes, has been the most commonly used experimental technique to study the kinetics and mechanisms of cure reactions of epoxy resins with different curing agents.^{41–43} A DSC thermogravimetric analysis Instrument Q20 DSC (TA Instruments, New Castle, DE) was used for calorimetric experiments. Owing to the wide range of temperature (190–260°C) necessary for this study, the calorimeter was calibrated using two standards (indium and *MilliQ* water resistivity 18.2 M Ω -cm at 25°C, Millipore Corporation, Billerica, MA). Analysis of data were made with OriginPro 7 (OriginLab Corporation, Northampton, MA).

Figure 2 shows an example of a DSC scan at a heating rate of 10°C min⁻¹ and at a 6 : 1 (epoxy/hemin) ratio. Table I shows some obtained results for the enthalpy at different stoichiometric ratios. It was found that the maximum enthalpy change was $\Delta H_{T,\max} = -488.3 \pm 8.4$ J g⁻¹ (average value from a minimum of seven experiments), corresponding to a 6 : 1 stoichiometric ratio. The negative value of the enthalpy indicates that an exothermic process is taken place. The use of compositions above 6 : 1 (mol/mol) results in a poor flow and increasing inhomogeneity of the mixtures affecting the molecular weight buildup, which in turn affects the adhesive properties.¹⁶ Furthermore, the DSC

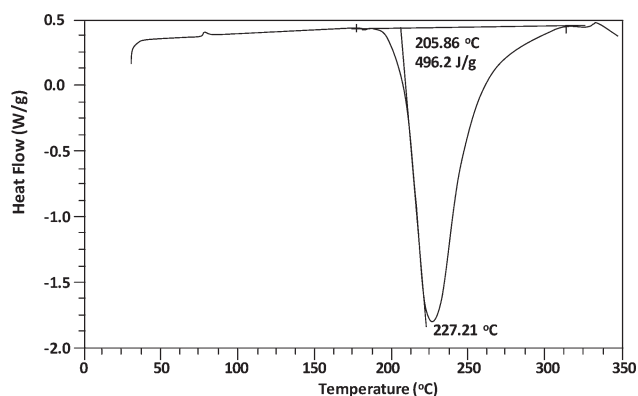


Figure 2. DSC scan at a heating rate of 10°C min⁻¹ and at a 6 : 1 ((BADGE, $n = 0$)/hemin) ratio.

Table I. Values of Enthalpy Changes at Different (BADGE, $n = 0$)/Hemin Ratios

(BADGE, $n = 0$)/hemin	ΔH_T (J g ⁻¹)
4 : 1	-440.5
5 : 1	-485.1
6 : 1	-488.3 ± 8.4
$n : 1$ ($n > 7$)	Asymmetric peaks

signal becomes increasingly asymmetric, probably due to competitive side effects.² For this reason, isothermal studies were conducted at 6 : 1 mixtures. The knowledge of the maximum enthalpy change⁴¹ is necessary for subsequent isothermal studies. A good knowledge of the cure kinetics allows one to determine suitable conditions for the structural formation of the material.

RESULTS AND DISCUSSION

Table II shows the obtained results for this system together with other data reported in the literature for similar systems. It can be noticed that $\Delta H_{T,\max}$ for this system is close to the average value.

To perform kinetic studies, the relationship between the extent of the reaction (or degree of conversion), α , is defined by the following equation:

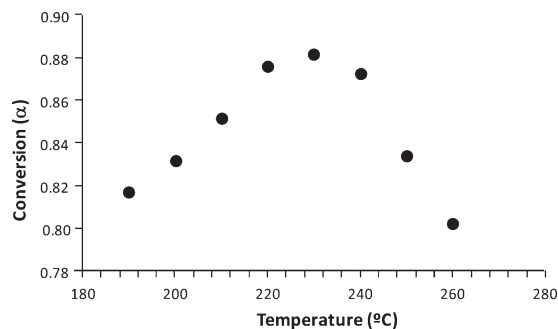
$$\alpha = \frac{\Delta H_T}{\Delta H_{T,\max}} \quad (1)$$

where ΔH_T is the heat evolved after infinite time at temperature T , and $\Delta H_{T,\max}$ is the value given above. ΔH_T values are determined from DSC experiments in an isothermal mode. Figure 3 shows α for the range 190–260°C used in this work, the maximum value being observed at $T_{\max} = 230^\circ\text{C}$. This interval of temperatures, high above the glass transition temperature, T_g , was selected since at temperatures close to T_g very low conversions were observed. The value for T_{\max} for the present system is comparable with the one observed for the (BADGE, $n = 0$)/Ni(II) chelate system³⁴ and higher than those observed for other systems in which the cross-linker is a diamine.^{5,44–46}

By assuming that the rate of heat released during cure at constant temperature is directly proportional to the rate of reaction, $d\alpha/dt$,⁴¹ the following equation may be written,

Table II. Values for $\Delta H_{T,\max}$ for the Cure of (BADGE, $n = 0$) with Various Cross-Linkers

Cross-linker	$\Delta H_{T,\max}$ (J g ⁻¹)	Reference
Hemin	-488.3 ± 8.4	This paper
Isophorone diamine	-519.5	5
1,2-Diamine cyclohexane	-400.15	44,45
1,2-Diamine cyclohexane with CaCO ₃ as filler	-324.17	44,45
Amantidine	-356	46
Ni(II) chelate system, Ni(en) ₃ I ₂	-707	34

**Figure 3.** Degree of conversion, α , of the epoxy (BADGE, $n = 0$)/hemin at different temperatures.

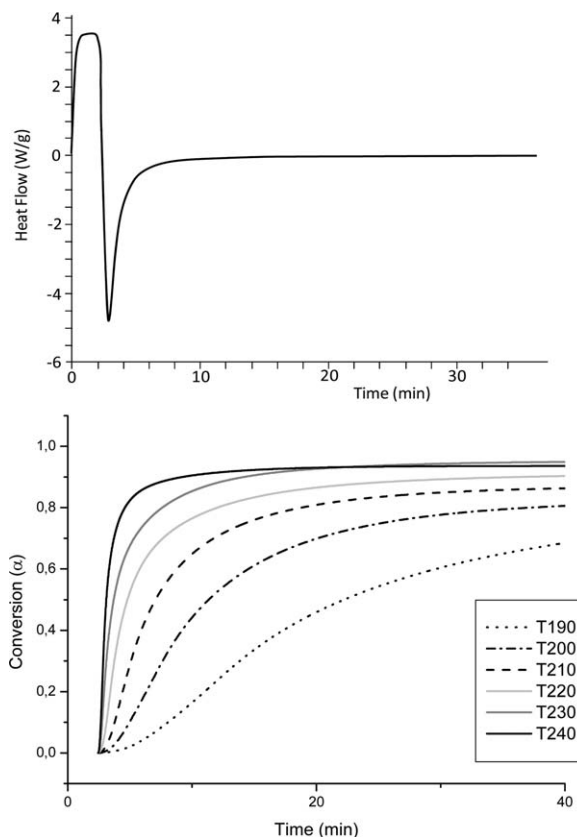
$$\frac{d\alpha}{dt} = \left(\frac{1}{\Delta H_T} \right) \left(\frac{dH}{dt} \right) \quad (2)$$

From previous equation, it is straightforward to deduce the degree of conversion,⁴⁶

$$\alpha = \frac{\int_{t_0}^t dH/dt}{\Delta H_T} \quad (3)$$

where t_0 is the initial time, and dH/dt is the rate of heat generation.

Figure 4 (top) shows a typical heat flow vs time experiment at 230°C. A minimum can be observed at approx. 3 min. This

**Figure 4.** (Top) Heat flow versus time at constant temperature (230°C). (Bottom) Degree of conversion versus time at different isothermal temperatures (values in the inset in °C).

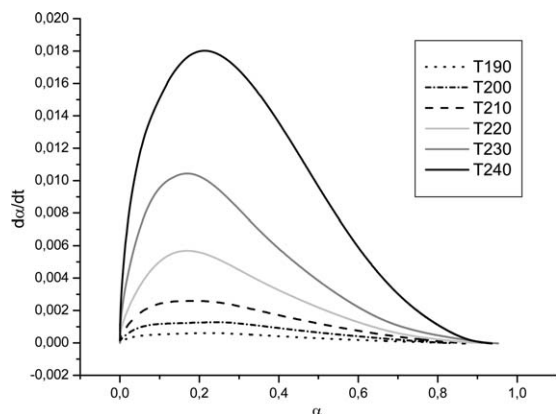


Figure 5. Reaction rate versus conversion plots for the different isothermal temperatures. Values in the inset in °C.

minimum corresponds to the maximum heat flow released during the reaction, and from that point, the power increases reaching a plateau at zero flow. These results are converted into the degree of conversion as indicated above. Figure 4 (bottom) shows the degree of conversion as a function of time at different temperatures. At all temperatures, it can be observed that conversion rapidly increases with curing time, reaching a constant value.

Figure 5 shows plots of the reaction rate vs the degree of conversion at different curing temperatures. It can be noticed that the reaction rate increases with temperature and that all curves show a maximum which is also dependent on temperature. Similar profiles have been observed for other (BADGE, $n = 0$) systems.^{5,46} This behavior suggests that Kamal⁴⁷ cure reaction model may be used for determining the kinetic coefficients and the global order of the cure reaction. The model has been largely used in the literature.^{5,46}

According to this model, the cure reaction rate is given by the following equation:

$$\frac{d\alpha}{dt} = k_1 (1-\alpha)^n + k_2 \alpha^m (1-\alpha)^n \quad (4)$$

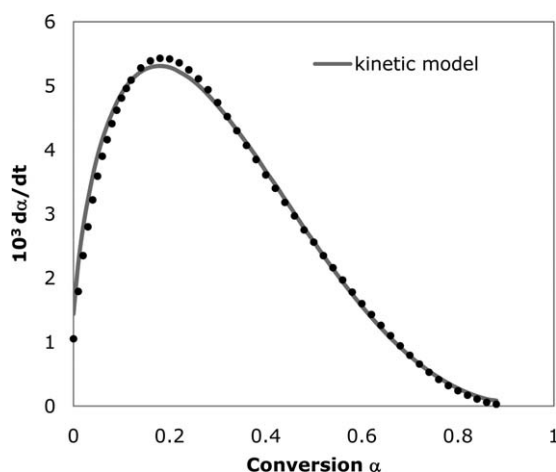


Figure 6. Reaction rate versus the degree of conversion at 220°C. The experimental results are compared with those obtained with the chemical kinetic model. Only a few experimental points are plotted.

where the first term is known as n -order mechanism and the second one as autocatalytic mechanism. k_1 and k_2 are the kinetic constants, and n and m are the reaction orders.

Figure 6 shows an example of the fitting of the experimental results at 220°C to previous equation. It can be noticed that the agreement between the experimental results and chemical kinetic model is extremely good, meaning that the cure reaction of this system is controlled by a chemical kinetics mechanism. When systematic deviations between theoretical model and experimental data increase with the conversion degree above a given value (usually taken as 58%, and known as critical conversion),⁴⁸ it is necessary to take into consideration the increasing effect of the physical diffusion on the process. Examples of the diffusion effect are well documented in literature.^{5,43,45,49–51} In these examples, as chains start branching and cross-linking, the viscosity of the medium increases and the mobility of the reacting groups is hindered.⁵² Thus the inexistence of systematic deviations allows one to conclude that diffusion is not significant in controlling the reaction rate in this system.

Table III shows the values obtained for the kinetic parameters at different curing temperatures. It may be observed that k_1 and k_2 increase with temperature and $k_2 > k_1$ (Figure 7), k_2 exhibiting a stronger positive temperature dependency than k_1 (see below). The values listed in Table III suggest a value of 3 for the overall reaction order ($m + n$). This is in agreement with reported values for the cure kinetics of this epoxy resin with adamantane,⁴⁶ and 1,2-diamine cyclohexane in the absence⁴⁴ and in the presence of calcium carbonate filler.⁴³ For the cure kinetics of this epoxy resin with isophorone diamine, an overall reaction order equal to two has been found.⁵

The activation energies corresponding to the n th order and autocatalyzed kinetic mechanisms were obtained from the Arrhenius plot (Figure 8, left). Values of activation energies are shown in Table IV. The activation energy for the autocatalyzed reaction is higher than the one for the n th-order path explaining the increase in the k_2/k_1 ratio with temperature (Figure 7).

The dependence of the kinetic constants with temperature is also commonly analyzed by application of the transition state theory. According to this theory, the kinetic constant is related

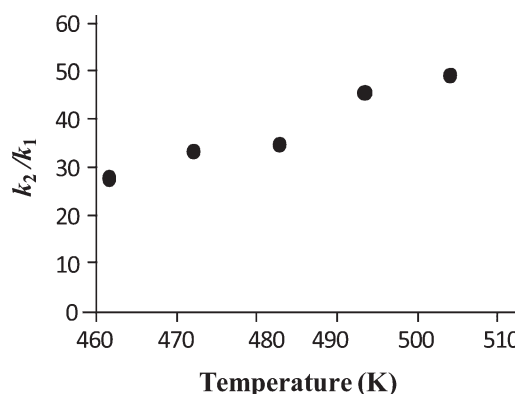
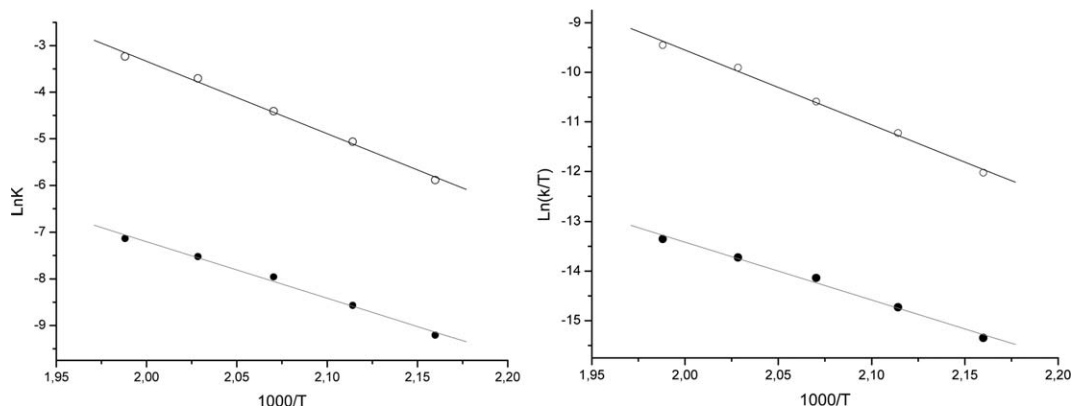


Figure 7. Ratio of the two kinetic constants, k_2 and k_1 , versus temperature.

Table III. Constant Rates and Reaction Orders for the Autocatalyzed and n th Order Mechanisms at Different Curing Temperatures

T (°C)	$10^4 k_1$ (min $^{-1}$)	$10^3 k_2$ (min $^{-1}$)	m	n	Overall reaction order ($m + n$)
190	1.0 ± 0.01	2.78 ± 0.01	0.636 ± 0.002	2.756 ± 0.005	3.40
200	1.9 ^a	6.31 ± 0.02	0.663 ± 0.003	2.7 ^a	3.36
210	3.5 ^a	12.2 ± 0.1	0.634 ± 0.002	2.752 ± 0.005	3.38
220	5.4 ± 0.7	24.6 ± 0.2	0.652 ± 0.008	2.7 ^a	3.35
230	8.0 ^a	39.4 ± 0.5	0.542 ± 0.007	2.87 ^a	3.41

^aThis parameter was kept constant during the fitting process.

**Figure 8.** Arrhenius plots (left) and transition state theory (right) plots for the autocatalytic (O) and n th order reaction pathways (•).

to the equilibrium constant for the formation of the transition state, K^\ddagger , by the equations

$$\Delta G^\ddagger = -RT \ln K = \Delta H^\ddagger - T\Delta S^\ddagger \quad (5)$$

$$\ln \frac{k}{T} = \ln \left(\frac{k_B}{h} e^{\frac{\Delta S^\ddagger}{R}} \right) - \frac{\Delta H^\ddagger}{RT} \quad (6)$$

where k_B and h are Boltzmann and Planck constants, respectively, R is the gas constant, ΔH^\ddagger is the activation heat of

reaction, and ΔS^\ddagger the entropy change of activation. From the plot of $\ln k/T$ against T^{-1} , (Figure 8, right) ΔH^\ddagger and ΔS^\ddagger are determined. Values of these thermodynamic parameters are shown in Table IV. ΔH^\ddagger is more negative for the autocatalytic reaction, and the activation energy is less positive, in agreement with previous studies of similar systems.^{33,34} The opposite case has also been found.^{5,44} Table IV also shows some experimental data found in the literature. When comparing with other systems, it can be noticed that the all thermodynamic activation

Table IV. Values of Activation Energies from Arrhenius Plot, and Thermodynamic Parameters for Activated Complex Formation Corresponding to the n th Order and Autocatalyzed Kinetic Mechanisms for Different BADGE/Cross-Linker Systems

Cross-linker	Autocatalytic mechanism			n th order mechanism			Reference
	ΔH^\ddagger	ΔS^\ddagger	E_a	ΔH^\ddagger	ΔS^\ddagger	E_a	
Hemin	-125 ± 5	-188 ± 1	129 ± 5	-97 ± 5	-177 ± 1	101 ± 5	This paper
1,2-Diamine cyclohexane	-44.7	-131	47.7	-58.3	-104	61.2	44
1,2-Diamine cyclohexane/filler	-54.4	-109	52.4	-71.8	-75.7	71.8	45
Isophorone diamine	-53.5	-155	56.3	-76.1	-77.8	59.0	5
Ni(II) chelate with ethylenediamine	-73.4	-102	77.0	-50.2	-178	53.8	33
Nickel with diethylenetriamine	-71.1	-162		-29.6	-255		34
4,4'-Diamino-azobenzene							
Reinforced with nanosilica	51.5	-161	55.2	70.2	-155	74.1	53
Reinforced with nanoclay	54.2	-160	58.2	99.6	-97.9	103	

E_a (kJ mol $^{-1}$), ΔH^\ddagger (kJ mol $^{-1}$), and ΔS^\ddagger (J mol $^{-1}$ K $^{-1}$).

parameters for this system are the highest ones which is in agreement with the highest T_{\max} mentioned above. Table IV also suggests that the values for the BADGE/4,4'-diaminoazobenzene system⁵³ are anomalous.

When ΔH^\ddagger and ΔS^\ddagger are both negative, below the temperature $T_o = \Delta H^\ddagger/\Delta S^\ddagger$, K^\ddagger will be >1 and above T_o , the equilibrium constant will be $K^\ddagger < 1$. T_o has been graphically illustrated for the autocatalytic process for the polymerization of BADGE with a nickel catalyst of diethylenetriamine.³⁴ The exactitude in the calculation of T_o depends on the exactitude of the values for the thermodynamic activation parameters. The calculation of the activation entropy is a highly uncertain procedure because its calculation requires an extrapolation of the experimental data far outside the range of available experimental temperatures. Consequently, the risk of obtaining wrong values is very high. We would like to remind that this type of uncertainty is also common for many enthalpy–entropy compensation plots proposed for several processes as for instance enzymatic catalysis.⁵⁴

With all these cautions in mind, from Table IV a value of 550 K is obtained for the autocatalytic process for the present system. This value is 37°C outside the range of experimental temperatures (190–240°C). T_o for the n th order mechanism is even farer away of such interval. From the thermodynamic parameters shown at Table IV, T_o may be calculated for the other systems, the values being in the range 347–551 K.

CONCLUSIONS

It has been demonstrated that hemin can be used as cross-linking agent for the cure for epoxy resins, allowing the introduction of iron in the network structure of the resin (BADGE, $n = 0$). The ratio between the corresponding kinetic constants and values of the Gibbs free energy changes for the n th path and autocatalytic mechanisms suggested a trend to the autocatalytic mechanism with increasing temperatures. No diffusion effects have been observed. Because of its high reactivity in a wide range of temperatures, the epoxy system studied here can be very useful for applications in different industries. Further work with other metallomacrocycles is in progress.

ACKNOWLEDGMENTS

The authors thank the Ministerio de Ciencia y Tecnología, Spain, Project MAT2010-61721 for financial support. ECV also thanks Dr. Senén Paz and GAIRESA for a scholarship.

REFERENCES

1. Pascault, J. P.; Williams, R. J. J. In *Epoxy Polymers. New Materials and Innovations*; Pascault, J.-P. a. W., Roberto J. J., Eds.; Wiley-VCH: Weinheim, Germany, **2010**, p 1.
2. Blank, W. J.; He, Z. A.; Picci, M. International Waterborne, High-Solids and Powder Coatings Symposium, February 21–23, 2001, New Orleans, LA, **2001**.
3. Fraga, F.; Burgo, S.; Rodríguez-Núñez, E. *J. Appl. Polym. Sci.* **2001**, *82*, 3366.
4. Fraga, F.; Castro-Díaz, C.; Rodríguez-Núñez, E.; Martínez-Ageitos, J. M. *J. Appl. Polym. Sci.* **2005**, *96*, 1591.
5. Fraga, F.; Penas, M.; Castro, C.; Rodríguez-Núñez, E.; Martínez-Ageitos, J. M. *J. Appl. Polym. Sci.* **2007**, *106*, 4169.
6. Martínez, P. A.; Cádiz, V.; Serra, A.; Mantecón, A. *Angew. Makromol. Chem.* **1985**, *136*, 159.
7. Serra, A.; Cádiz, V.; Martínez, P. A.; Mantecón, A. *Makromol. Chem.* **1986**, *187*, 1907.
8. Mantecón, A.; Cádiz, V.; Serra, A.; Martínez, P. A. *Eur. Polym. J.* **1987**, *23*, 481.
9. Shechter, L.; Wynstra, J.; Kurkijy, R. P. *Ind. Eng. Chem.* **1957**, *49*, 1107.
10. Alvey, F. B. *J. Polym. Sci. A-1* **1969**, *7*, 2117.
11. Serra, A.; Cádiz, V.; Mantecón, A. *Angew. Makromol. Chem.* **1987**, *155*, 93.
12. Mang, M. N.; White, J. E.; Haag, A. P.; Kram, S. L.; Brown, C. N. *Polymer Preprints* **1995**, *36*, 180.
13. Galia, M.; Monte, D.; Serra, A.; Mantecón, A.; Cádiz, V. *J. Appl. Polym. Sci.* **1996**, *60*, 2177.
14. Yang, J. I. Synthesis of aromatic polyketones via soluble precursors derived from Bis(A-Amininitrile)s. Modifications of epoxy resins with functional hyperbranched poly(arylene ester)s, PhD, Virginia Polytechnic Institute and State University, **1998**, Chapter 11.
15. Chin, W.-K.; Hwu, J.-J.; Shau, M.-D. *Polymer* **1998**, *39*, 4923.
16. Abraham, G.; Packirisamy, S.; Vijayan, T. M.; Ramaswamy, R. *J. Appl. Polym. Sci.* **2003**, *88*, 1737.
17. Patel, H. S.; Panchal, K. K. *E-J. Chem.* **2004**, *1*, 32.
18. Patel, H. S.; Panchal, K. K. *Int. J. Polym. Mater.* **2005**, *54*, 1.
19. Singh, D.; Narula, A. K. *J. Thermal Anal. Cal.* **2010**, *100*, 199.
20. Thakkar, J. R. *Int. J. Polym. Mater. Polym. Biomater.* **1995**, *29*.
21. Pedersen, C. J. *J. Am. Chem. Soc.* **1967**, *89*, 7017.
22. Lehn, J.-M. *Supramolecular Chemistry*; VCH: Weinheim, Germany, **1995**.
23. Cragg, P. A. *Practical Guide to Supramolecular Chemistry*; Wiley: New York, **2005**.
24. Bourre, L.; Thibaut, S.; Briffaud, A.; Lajat, Y.; Patrice, T. *Pharmacol. Res.* **2002**, *45*, 159.
25. Zaytsev, D. V.; Xie, F.; Mukherjee, M.; Bludín, A.; Demeler, B.; Breece, R. M.; Tierney, D. L.; Ogawa, M. Y. *Biomacromolecules* **2010**, *11*, 2602.
26. Chou, J.-H.; Kosal, M. E.; Nalwa, H. S.; Rakow, N. A.; Suslick, K. S. In *Porphyrim Handbook*; Kadish, K., Smith, K., Guilard, R., Eds.; Academic Press: New York, **2000**; Vol. 6, p 43.
27. Li, F.; Yang, S. I.; Ciringh, Y.; Seth, J.; Martin, C. H., III; Singh, D. L.; Kim, D.; Birge, R. R.; Bocian, D. F.; Holten, D. e. a. *J. Am. Chem. Soc.* **1998**, *120*, 10001.
28. Takahashi, R.; Kobuke, Y. *J. Am. Chem. Soc.* **2003**, *125*, 2372.
29. Brown, J.; Hamerton, I.; Howlin, B. J. *J. Appl. Polym. Sci.* **2001**, *75*, 201.

30. Hamerton, I.; Hay, J. N.; Howlin, B. J.; Jepson, P.; Mortimer, S. *J. Appl. Polym. Sci.* **2001**, *80*, 1489.1503.
31. Hamerton, I.; Hay, J. N.; Herman, H.; Howlin, B. J.; Jepson, P.; Gillies, D. G. *J. Appl. Polym. Sci.* **2002**, *84*, 2411.
32. Ghaemy, M.; Omrani, A.; Rostami, A. A. *J. Appl. Polym. Sci.* **2005**, *97*, 265.
33. Ghaemy, M.; Omrani, A.; Rostami, A. A. *J. Appl. Polym. Sci.* **2005**, *98*, 1540.
34. Ghaemy, M.; Rostami, A. A.; Omrani, A. *Polym. Int.* **2006**, *55*, 279.
35. Kurnoskin, A. V. *J. Appl. Polym. Sci.* **1992**, *46*, 1509.
36. Kurnoskin, A. V. *Ind. Eng. Chem. Res.* **1992**, *31*, 524.
37. Kurnoskin, A. V. *Polym. Composites* **1993**, *14*, 481.
38. Kurnoskin, A. V. *J. Macromol. Sci. C* **1996**, *C36*, 457.
39. Yu, H.; Wang, L.; Huo, J.; Ding, J.; Tan, Q. *J. Appl. Polym. Sci.* **2008**, *110*, 1594.
40. Takano, T.; Musa, O. M. Patent WO 2008111980 A1 20080918, 2008.
41. Núñez, L.; Fraga, F.; Fraga, L.; Salgado, T.; Rodríguez Añón, J. *Pure Appl. Chem.* **1995**, *67*, 1091.
42. Riccardi, C. C.; Fraga, F.; Dupuy, J.; Williams, R. J. *J. Appl. Polym. Sci.* **2001**, *82*, 2319.
43. Fraga, F.; Vázquez, I.; Rodríguez Núñez, E.; Martínez-Ageitos, J. M.; Miragaya, J. *J. Appl. Polym. Sci.* **2009**, *114*, 3338.
44. Núñez, L.; Fraga, F.; Fraga, L.; Castro, A. *J. Appl. Polym. Sci.* **1997**, *63*, 635.
45. Núñez, L.; Fraga, F.; Castro, A.; Núñez, M. R.; Villanueva, M. *J. Appl. Polym. Sci.* **2000**, *75*, 291.
46. Fraga, F.; Soto, V. H.; Rodríguez Núñez, E.; Martínez-Ageitos, J. M.; Rodríguez, V. J. *Therm. Anal. Calorim.* **2007**, *87*, 97.
47. Kamal, M. R. *Polym. Eng. Sci.* **1974**, *14*, 230.
48. Flory, P. L. Principles of Polymer Chemistry, 15th ed.; Cornell Uni. Press: Ithaca, NY, **1992**.
49. Cole, K. C.; Hechler, J. J.; Noel, D. *Macromolecules* **1991**, *24*, 3098.
50. Khanna, U.; Chanda, M. *J. Appl. Polym. Sci.* **1993**, *49*, 319.
51. Núñez, L.; Fraga, F.; Núñez, M. R.; Fraga, L. *J. Appl. Polym. Sci.* **1999**, *74*, 2997.
52. Núñez, L.; Fraga, F.; Castro, A.; Núñez, M. R.; Villanueva, M. *J. Appl. Polym. Sci.* **2000**, *77*, 2285.
53. Barghamadi, M. *Polym. Composites* **2010**, *31*, 1442.
54. Cornish-Bowden, A. *J. Biosci.* **2002**, *27*, 121.